8. B. C. Sakiadis, Boundary layer behaviour on continuous solid surface: II. Boundary layer equations on continuous surface, *A.I.Ch.E. Jl* **7**, 221–225 (1961).

APPENDIX: INTEGRAL ANALYSIS

An integral of momentum equation (12) between limits zero to ∞ gives

$$f''(0) = \int_0^\infty \varepsilon f' - f'^2 \, d\eta. \tag{A1}$$

Introducing a function ϕ such that

$$\phi(\zeta) = \frac{u-U_w}{U_\infty - U_w} = \frac{f'+\varepsilon-1}{2\varepsilon-1}, \quad \zeta = \frac{\eta}{A} \tag{A2}$$

$$\phi(0) = 0, \quad \phi(\infty) = 1.$$

The momentum integral (A1) yields

$$A^2 = \phi'(0)/[B_1 - B_2 - \varepsilon(B_1 - 2B_2)] \tag{A3}$$

where

$$B_1 = \int_0^\infty 1-\phi \, d\zeta, \quad B_2 = \int_0^\infty \phi - \phi^2 \, d\zeta.$$

Using the above results it can be shown that

$$f''(0) = (2\varepsilon-1)[\phi'(0)(B_1 - B_2 - \varepsilon(B_1 - 2B_2))]^{1/2}$$

$$b = (2\varepsilon-1)B_1 A. \tag{A4}$$

The relation (A4) shows that a solution does not exist for $\varepsilon > \varepsilon_0$ where ε_0 is given by

$$\varepsilon_0 = 1 + (H-2)^{-1} \tag{A5}$$

where $H = B_1/B_2$ is the shape factor ($H > 2$, $\varepsilon_0 > 1$).

If one considers a trial velocity profile

$$\phi(\zeta) = (3\zeta - \zeta^3)/2, \quad \zeta \leqslant 1; \quad \phi(\zeta) = 1, \quad \zeta > 1$$

$$B_1 = 3/8, \quad B_2 = 39/280$$

then $\varepsilon_0 = 2.46$ and the solution is given by

$$f''(0) = (2\varepsilon-1)(0.3536 - 0.1446\varepsilon)^{1/2} \tag{A6}$$

and for the trial profile

$$\phi(\zeta) = 2\zeta - 2\zeta^3 + \zeta^4, \quad \zeta \leqslant 1; \quad \phi(\zeta) = 1, \quad \zeta > 1$$

$$B_1 = 3/10, \quad B_2 = 37/315$$

$\varepsilon_0 = 2.81$ and the solution is given by

$$f''(0) = (2\varepsilon-1)(0.365 - 0.130\varepsilon)^{1/2}. \tag{A7}$$

The expression (A7) includes the two results (10) and (18) of ref. [2] as special cases. These solutions are good for $\varepsilon \leqslant 1$ as for $\varepsilon = 1$ the error is about 2% and $\varepsilon = 0$ the error is about 5%. As $\varepsilon \to -\infty$, the asymptotic behaviour of integral solution (A7) leads to

$$f''(0) \to -0.72(-\varepsilon)^{3/2}$$

$$b \to -0.83(-\varepsilon)^{1/2}. \tag{A8}$$

Int. J. Heat Mass Transfer. Vol. 36, No. 13, pp. 3403–3406, 1993
Printed in Great Britain

0017–9310/93 $6.00 + 0.00

Three-dimensional natural convection in a vertical porous layer with hexagonal honeycomb core of negligible thickness

YOSHIYUKI YAMAGUCHI, YUTAKA ASAKO and HIROSHI NAKAMURA
Department of Mechanical Engineering, Tokyo Metropolitan University, Tokyo 192-03, Japan

and

MOHAMMAD FAGHRI
Department of Mechanical Engineering, University of Rhode Island, Kingston, RI 02881, U.S.A.

(*Received* 15 *October* 1991 *and in final form* 30 *September* 1992)

INTRODUCTION

HONEYCOMB structures are often used in thermal insulating walls. Inside such walls, the main mechanisms of heat transfer are by natural convection and radiation. A number of studies for natural convection heat transfer in such an air layer were investigated by Asako *et al.* [1–3]. If the air layer is filled with thermal insulations, such as glass wool, both convective and radiative heat transfer rates will decrease. A numerical analysis was reported by Asako *et al.* [4] to investigate heat transfer characteristics by natural convection in such a porous layer. The results were obtained for both conductive and adiabatic honeycomb core wall thermal boundary conditions. These conditions exist when the honeycomb core walls are good conductors and thick, and also when they are thermally insulated. For thermal insulating walls, it is required to reduce the heat loss through the honeycomb core walls. Then, the honeycomb core walls should be made as thin as possible to reduce the heat conduction through it. The motivation for the present study is to analyse the case where the honeycomb core walls are assumed to be poor conductors and thin, such that the thermal wall boundary conditions approach the so-called 'no-thickness' wall boundary condition dictated by Nakamura *et al.* [5]. These three boundary conditions, 'conduction', 'adiabatic', and 'no-thickness', can be considered as three idealized thermal boundary conditions. Therefore, the heat transfer rate in a practical porous layer will have a value that lies within these three conditions.

The numerical methodology used in this study utilizes an

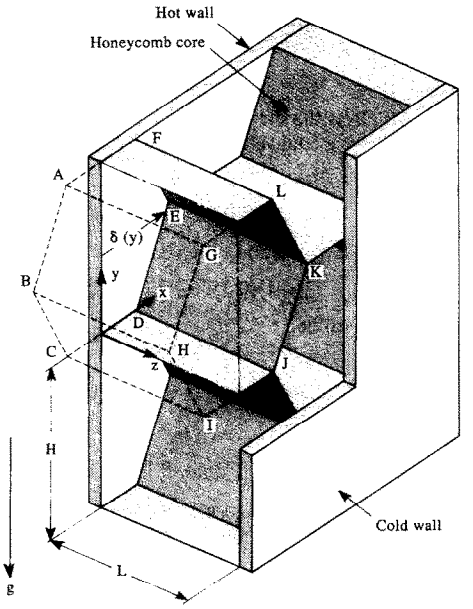

FIG. 1. Schematic diagram of a vertical porous layer with honeycomb core.

algebraic coordinate transformation technique developed by Faghri *et al.* [6], which maps an irregular cross-section into a rectangle. This method was extended to three-dimensional problems by Asako *et al.* [1]. In this note, the flow is obtained using the Darcian model, and the porous layer is assumed to be homogeneous and isotropic. The numerical solutions were obtained for a range of the Darcy–Rayleigh numbers from 10 to 1000 and for a range of aspect ratios from 0.25 to 5. Unfortunately, no experimental results are available for comparison with the present work. However, the results of this work are compared with the corresponding values for two-dimensional rectangular enclosures.

FORMULATION

Description of the problem

The problem considered in this study is schematically depicted in Fig. 1. It involves the determination of three-dimensional heat transfer for natural convection in a vertical porous layer with a hexagonal honeycomb core. If the porous layer is very long and wide in both the vertical and the horizontal directions, the velocity and temperature fields repeat themselves in successive enclosures except at the end boundaries of the layer. Therefore, it is possible to solve the natural convection problem in only one hexagonal honeycomb porous enclosure with an appropriate thermal boundary condition. As seen in Fig. 1, the two hexagonal end walls of the enclosure are kept at uniform temperatures t_H and t_C, respectively. The honeycomb core walls (the side walls) can be modeled as poor conductors and thin. The geometry of the problem is specified by the height (H) and the length (L). The solution domain, with the assumption of symmetry, is confined to the right half of the honeycomb enclosure. The mathematical expression for the width of this honeycomb, $\delta(y)$, is given in an earlier paper by Asako *et al.* [1].

The conservation equations

The governing equations are the continuity and energy equations. The flow field is approximated by the Darcian model. Constant thermophysical properties are assumed except for the density in the buoyancy force term. The following dimensionless variables are used:

$$X = x/L, \quad Y = y/L, \quad Z = z/L,$$
$$U = u/(a/L), \quad V = v/(a/L), \quad W = w/(a/L),$$
$$P = pK/a\mu, \quad T = (t-t_m)/(t_H-t_C),$$
$$Ra^* = Kg\beta_f L(t_H-t_C)/av \tag{1}$$

where t_m is the average temperature of the end walls and is expressed by $t_m = (t_H+t_C)/2$. Then, upon introduction of dimensionless variables and parameters, for steady natural convection in a porous medium, the governing equations take the following forms:

$$\partial U/\partial X+\partial V/\partial Y+\partial W/\partial Z = 0 \tag{2}$$
$$U = -\partial P/\partial X \tag{3}$$
$$V = -\partial P/\partial Y+Ra^* T \tag{4}$$
$$W = -\partial P/\partial Z \tag{5}$$
$$U(\partial T/\partial X)+V(\partial T/\partial Y)+W(\partial T/\partial Z) = \nabla^2 T \tag{6}$$

where

$$\nabla^2 = \partial^2/\partial X^2+\partial^2/\partial Y^2+\partial^2/\partial Z^2. \tag{7}$$

To complete the formulation of the problem, the necessary boundary conditions are discussed below

$$\text{at all walls: } \mathbf{V}\cdot\mathbf{N} = 0$$

and at the symmetry plane ($X = 0$):

$$U = \partial V/\partial X = \partial W/\partial X = 0. \tag{8}$$

Here, **V** and **N** are the velocity vector and the normal vector to the walls, respectively. The non-permeable boundary condition is attributed to the wall. Therefore, the thermal boundary conditions on the hot and cold walls reduce to

$$\text{hot wall: } T = 0.5$$
$$\text{cold wall: } T = -0.5. \tag{9}$$

The thermal boundary condition for the side walls is the 'no-thickness' wall condition, which assumes that conduction is negligible along the walls (the horizontal direction), because they are thin. Therefore, the heat flux through the top wall (AGLF) becomes equal to that through the bottom wall (CIJD); the heat flux through one of the upper side walls (ABHG) becomes equal to that through the lower side wall (EDJK). From the assumption of symmetry, the heat flux through the right upper wall (FEKL) becomes equal to that through the left side wall (ABHG). The mathematical expressions for these conditions are expressed as follows:

$$T_{AGLF} = T_{CIJD}, \quad (\partial T/\partial N)_{AGLF} = -(\partial T/\partial N)_{CIJD}$$
$$T_{EFKL} = T_{EDJK}, \quad (\partial T/\partial N)_{EFKL} = -(\partial T/\partial N)_{EDJK}. \tag{10}$$

Here, N is the dimensionless coordinate directed along the outward normal to the walls.

Numerical methods

A simple algebraic coordinate transformation is used which maps the hexagonal cross-section onto a rectangle. Specifically, the X, Y coordinates are transformed into η, ξ coordinates by the following relations:

$$\eta = X/[\delta(y)/L], \quad \xi = Y. \tag{11}$$

In terms of the new coordinates, the solution domain is defined by $0 < \eta < 1$, $0 < \xi < H/L$. The transformed equations, their discretization and solutions, are documented in an earlier paper by Asako *et al.* [4]. The discretized equations for the thermal boundary conditions and their numerical implementation have been documented in an earlier paper by Asako *et al.* [2]. The discretized procedure of the equations is based on the control volume technique, using the power-law scheme of Patankar [7], and the discretized equations are solved by using a line-by-line method. The pressure and

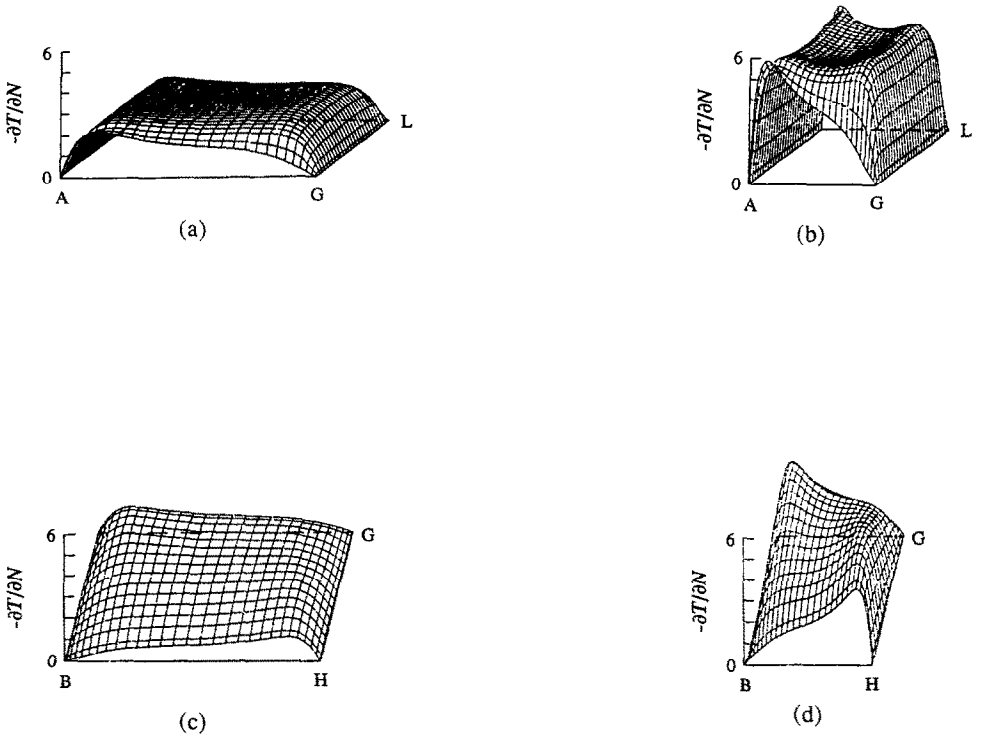

FIG. 2. Heat flow through the side wall for $Ra^* = 100$: (a) top wall for $H/L = 1$; (b) top wall for $H/L = 2$; (c) upper side wall for $H/L = 1$; (d) upper side wall for $H/L = 2$.

velocities are linked by the SIMPLE algorithm of Patankar [8]. Note that the SIMPLE algorithm for the pressure–velocity linkage for the Darcian model can be considered as an implicit method rather than a semi-implicit method. Because of this, a good convergence was obtained.

The computations were performed with $(16 \times 22 \times 22)$, $(16 \times 30 \times 30)$, and $(16 \times 40 \times 40)$ grid points, for $Ra^* = 10$, 100 and 1000, respectively. The grid points were uniformly distributed in the η and ξ directions, but non-uniformly in the Z direction with a higher concentration near the hexagonal end walls. The effect of grid size on the Nusselt number has already been examined and illustrated in the previous paper by Asako *et al.* [4].

From an examination of the governing equations (2)–(6), it can be seen that there is only one flow parameter whose value has to be specified prior to the initiation of the numerical solution. This is the Darcy–Rayleigh number, Ra^*. In this paper, the values chosen for this parameter are in the range from 10 to 1000. Aside from Ra^*, there are two geometric parameters which have to be specified. These are the height (H) and the length (L) of the enclosure. If L is used as a reference length, then H/L needs to be specified as the geometric parameter. The selected values for H/L were 0.25, 0.333, 0.5, 0.7, 1, 1.4, 2 and 5, respectively.

Nusselt numbers

The local and average heat transfer coefficients on the hot wall are defined as

$$h = q/(t_H - t_C) \tag{12}$$

$$h_m = Q/[A_H(t_H - t_C)] \tag{13}$$

where q is the local heat flux, A_H the area of the hexagonal

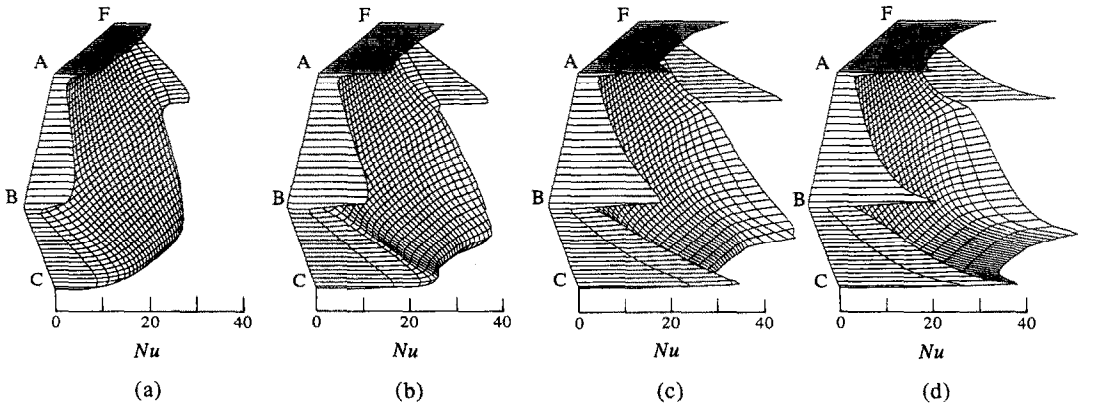

FIG. 3. Local Nusselt number on the hot wall for $Ra^* = 1000$: (a) $H/L = 0.5$; (b) $H/L = 1$; (c) $H/L = 2$; (d) $H/L = 5$.

hot wall equal to $(3/2)H^2 \tan(\pi/6)$ and Q the total heat transfer rate from the hot wall. The expressions for the Nusselt number are given below

$$Nu = hL/k = -(\partial T/\partial Z)_{H} \quad (14)$$

$$Nu_m = h_m L/k = -2\int_0^{H/L}\int_0^1 (\partial T/\partial Z)_H(\delta/L)\,d\eta\,d\xi \Big/ [(3/2)(H/L)^2 \tan(\pi/6)]. \quad (15)$$

RESULTS AND DISCUSSION

Heat flux through side walls

The heat flux through the top side wall (AGLF) and the upper side wall (ABHG) are presented in Figs. 2(a) and (c), respectively, for $H/L = 1$ and $Ra^* = 100$, and in Figs. 2(b) and (d) for $H/L = 2$ and $Ra^* = 100$. As seen from these figures, the dimensionless value of the heat flux, $(-\partial T/\partial N)$, always takes a positive value. This indicates that the direction of the heat flow which passes through the top and upper side walls is upward. The value of $(-\partial T/\partial N)$ increases with increasing aspect ratio.

Local Nusselt number

The local Nusselt numbers on the hot wall for $Ra^* = 1000$ are presented in Fig. 3. In this figure, the Nusselt numbers for the aspect ratios 0.5, 1, 2, 5 are shown in (a), (b), (c) and (d), respectively. The local Nusselt numbers for $H/L = 0.25$ approach unity, and in the case of a low aspect ratio ($H/L = 0.5$), the local Nusselt number takes the highest value on the symmetry line. The Nusselt number profile changes with increasing values of the aspect ratio and it has two peaks which move to lower corners of the hot wall with increasing aspect ratios.

Average Nusselt number

The average Nusselt numbers, Nu_m, are plotted as a function of the aspect ratio, H/L, with the Darcy–Rayleigh number as a curve parameter in Fig. 4. The values of Nu_m for $Ra^* = 10$ approach unity and are not plotted here. The Nusselt numbers for conductive and adiabatic side wall conditions are also plotted in this figure. As seen from this figure, the Nusselt number for the 'no-thickness' boundary condition takes a value between the values for conductive and adiabatic side wall boundary conditions.

The dashed lines in the figure are the result for a two-dimensional rectangular enclosure of height H and horizontal length L. The full three-dimensional computation requires excessive computing time. Therefore, it would be helpful if the average Nusselt number could be predicted from the result of a two-dimensional model. To investigate this, supplementary two-dimensional computations were performed with (40×40) grid points for $Ra^* = 1000$ and (30×30) grid points for $Ra^* = 100$, respectively. The grid point distribution is similar to those used for three-dimensional computations. Namely, the grid points were distributed uniformly along the vertical Y-direction, while non-uniformly along the horizontal Z-direction, with a higher concentration of the grid points near the hot and cold walls. Slight differences between a two-dimensional rectangular enclosure and the honeycomb enclosure can be seen in the figure for $Ra^* = 1000$ and for the lower aspect ratios.

CONCLUDING REMARKS

Three-dimensional natural convection heat transfer characteristics in a porous layer with a hexagonal honeycomb-core structure, of negligible thickness, have been obtained numerically by a coordinate transformation technique. The computations are performed for Darcy–Rayleigh numbers in the range of 10–1000 and for eight values of aspect ratio. The main conclusions are:

(a) the heat passes upward through the honeycomb core walls,

(b) the average Nusselt number for the 'no-thickness' boundary condition takes a value between those for the conductive and the adiabatic side wall thermal conditions, and

(c) the average Nusselt number can be predicted by a two-dimensional rectangular result, depending on the aspect ratio and the Darcy–Rayleigh number.

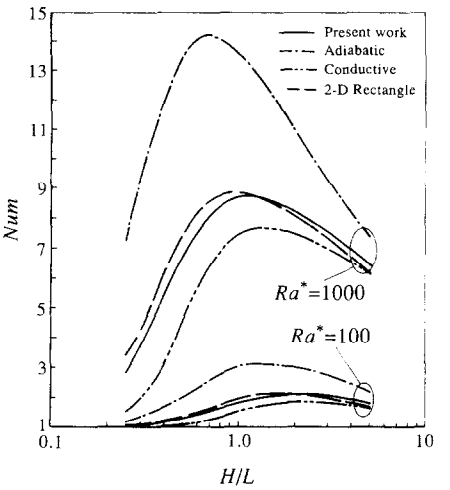

FIG. 4. Average Nusselt number, Nu_m, as a function of the aspect ratio, H/L.

REFERENCES

1. Y. Asako, H. Nakamura and M. Faghri, Three-dimensional laminar natural convection in a honeycomb enclosure with hexagonal end walls, *Numer. Heat Transfer* **15**, 67–86 (1989).
2. Y. Asako, H. Nakamura and M. Faghri, Three-dimensional laminar natural convection in a vertical air slot with hexagonal honeycomb core, *J. Heat Transfer* **112**, 130–136 (1990).
3. Y. Asako, H. Nakamura, Z. Chen and M. Faghri, Three-dimensional laminar natural convection in an inclined air slot with a hexagonal honeycomb core, *J. Heat Transfer* **113**, 19–24 (1991).
4. Y. Asako, H. Nakamura, Y. Yamaguchi and M. Faghri, Three-dimensional natural convection in a vertical porous layer with a hexagonal honeycomb core, *3rd ASME/JSME Thermal Engng Joint Conf.* Vol. 4, pp. 197–202 (1991).
5. H. Nakamura, Y. Asako and H. Aoki, Natural convection heat transfer in a vertical air slot partitioned by corrugated plates, *Numer. Heat Transfer* **11**, 77–94 (1987).
6. M. Faghri, E. M. Sparrow and A. T. Prata, Finite difference solutions of convection–diffusion problems in irregular domains using a non-orthogonal coordinate transformation, *Numer. Heat Transfer* **7**, 183–209 (1984).
7. S. V. Patankar, A calculation procedure for two-dimensional elliptic situations, *Numer. Heat Transfer* **4**, 409–425 (1981).
8. S. V. Patankar, *Numerical Heat Transfer and Fluid Flow*. Hemisphere, Washington, D.C. (1980).